

Higher Order Top Squark Decays

W. Porod¹, T. Wöhrmann²

¹ Institut für Theoretische Physik, Universität Wien, A-1090 Wien,
Austria

² Institut für Theoretische Physik, Universität Würzburg,
D-97074 Würzburg, Germany

Abstract

Within the Minimal Supersymmetric Standard Model we study the three body decay of the lighter top squark $\tilde{t}_1 \rightarrow bW\tilde{\chi}_1^0$ and compare this decay with the flavour changing two body decay $\tilde{t}_1 \rightarrow c\tilde{\chi}_1^0$. Here $\tilde{\chi}_1^0$ is the lightest neutralino which we assume to be the lightest supersymmetric particle (LSP). We do this for scenarios where two body decays at tree level are forbidden for the light top squark. We give the complete analysis for the three body decay and compare it with the mentioned two body decay. We discuss our numerical results in view of the upgraded Tevatron, the LHC and a 500 GeV e^+e^- Linear Collider.

August 1996

¹email:porod@merlin.pap.univie.ac.at

²email: woerman@physik.uni-wuerzburg.de

1 Introduction

Supersymmetry is considered as one of the most promising extensions of the standard model [1]. Its search is therefore an important part of the experimental program at current and future colliders, namely at the Tevatron, LEP1.5, LEP2, LHC and a prospective future 500 GeV e^+e^- Linear Collider.

Within the supersymmetric extensions of the standard model the minimal supersymmetric standard model (MSSM) [2, 3] is the most investigated one. It contains beside the known SM-particles spin 1/2 partners for the gauge bosons (bino, wino, zino, gluino), five physical Higgs bosons (two scalar h^0, H^0 , one pseudoscalar A^0 and two charged H^\pm) and their spin 1/2 partners (higgsinos). The $SU(2) \times U(1)$ interaction eigenstates bino, zino, wino and higgsinos mix leading to mass eigenstates called neutralinos $\tilde{\chi}_i^0$ ($i=1,2,3,4$) and charginos $\tilde{\chi}_j^\pm$ ($j=1,2$) (see e.g. [4] and references therein). Each fermion has two spin zero partners called sfermions \tilde{f}_L and \tilde{f}_R , one for each chirality eigenstate: the mixing between \tilde{f}_L and \tilde{f}_R is proportional to the corresponding *fermion* mass, and so negligible except for the third generation.

The main parameters for the following discussion are M' , M_2 , μ , $\tan\beta$, M_{D_i} , M_{Q_i} , M_{U_i} , A_{d_i} and A_{u_i} . M' (M_2) is the $U(1)$ ($SU(2)$) gaugino mass. In the following we will assume the GUT relation $M' = 5/3 \tan^2 \theta_W M_2$. μ is the parameter of the higgs potential and $\tan\beta = v_2/v_1$ where v_i denotes the vacuum expectation value of the Higgs doublet H_i . M_{D_i} , M_{Q_i} and M_{U_i} are soft SUSY breaking masses for the squarks, A_{d_i} and A_{u_i} are trilinear Higgs-squark couplings.

The mass matrix for squarks in the $(\tilde{f}_L, \tilde{f}_R)$ basis has the following form:

$$\mathcal{M}_{\tilde{f}_i}^2 = \begin{pmatrix} m_{\tilde{f}_{Li}}^2 & a_{f_i} m_{f_i} \\ a_{f_i} m_{f_i} & m_{\tilde{f}_{Ri}}^2 \end{pmatrix} \quad (1)$$

with

$$\begin{aligned} m_{\tilde{u}_{Li}}^2 &= M_{Q_i}^2 + m_{u_i}^2 + m_Z^2 \cos 2\beta \left(\frac{1}{2} - \frac{2}{3} \sin^2 \theta_W \right), \\ m_{\tilde{u}_{Ri}}^2 &= M_{U_i}^2 + m_{u_i}^2 + \frac{2}{3} m_Z^2 \cos 2\beta \sin^2 \theta_W, \\ m_{\tilde{d}_{Li}}^2 &= M_{Q_i}^2 + m_{d_i}^2 - m_Z^2 \cos 2\beta \left(\frac{1}{2} - \frac{1}{3} \sin^2 \theta_W \right), \\ m_{\tilde{d}_{Ri}}^2 &= M_{D_i}^2 + m_{d_i}^2 - \frac{1}{3} m_Z^2 \cos 2\beta \sin^2 \theta_W, \end{aligned} \quad (2)$$

and

$$a_{u_i} m_{u_i} = m_{u_i} (A_{u_i} - \mu \cot \beta), \quad a_{d_i} m_{d_i} = m_{d_i} (A_{d_i} - \mu \tan \beta) \quad (3)$$

where i is a generation index ($u_i = u, c, t$; $d_i = d, s, b$) which will be suppressed in the following.

The mass eigenstates \tilde{f}_1 and \tilde{f}_2 are related to \tilde{f}_L and \tilde{f}_R by:

$$\begin{pmatrix} \tilde{f}_1 \\ \tilde{f}_2 \end{pmatrix} = \begin{pmatrix} \cos \theta_f & \sin \theta_f \\ -\sin \theta_f & \cos \theta_f \end{pmatrix} \begin{pmatrix} \tilde{f}_L \\ \tilde{f}_R \end{pmatrix} \quad (4)$$

with the eigenvalues

$$m_{\tilde{f}_{1,2}}^2 = \frac{1}{2}(m_{\tilde{f}_L}^2 + m_{\tilde{f}_R}^2) \mp \frac{1}{2}\sqrt{(m_{\tilde{f}_L}^2 - m_{\tilde{f}_R}^2)^2 + 4a_f^2 m_f^2}. \quad (5)$$

The mixing angle θ_f is given by

$$\cos \theta_f = \frac{-a_f m_f}{\sqrt{(m_{\tilde{f}_L}^2 - m_{\tilde{f}_R}^2)^2 + a_f^2 m_f^2}}, \quad \sin \theta_f = \sqrt{\frac{(m_{\tilde{f}_L}^2 - m_{\tilde{f}_R}^2)^2}{(m_{\tilde{f}_L}^2 - m_{\tilde{f}_R}^2)^2 + a_f^2 m_f^2}}. \quad (6)$$

Analogous expressions are also valid for sleptons.

Due to the fact that the off-diagonal terms in eq. (1) and therefore $\cos \theta_f$ is proportional to the fermion mass the mixing can safely be neglected for the first two generations but in general not for the third generation. In particular one expects for the top squarks due to the huge top mass [5] a strong mixing and a possible big mass splitting with one light top squark. In the following the top squark (bottom squark) will be denoted by stop (sbottom).

In general sfermions decay according to $\tilde{f}_k \rightarrow \tilde{\chi}_i^0 f$ and $\tilde{f}_k \rightarrow \tilde{\chi}_j^\pm f'$, where we assume as usual that the $\tilde{\chi}_1^0$ is the lightest supersymmetric particle (LSP). Contrary to the other sfermions, where the flavour conserving decay into the lightest neutralino is always possible, the decay of the stop into the lightest neutralino will be kinematically forbidden for stop masses accessible at the Tevatron. Therefore the phenomenological analysis of stop signals is different from those of other squarks. Due to the big difference between the top mass and the bottom mass, even in many scenarios, where the decay $\tilde{t}_1 \rightarrow t\tilde{\chi}_1^0$ is kinematically forbidden, the decay into the b-quark and the lighter chargino, which is heavier than $\tilde{\chi}_1^0$, could still be possible. Since the lower mass limit of $\tilde{\chi}_1^+$ is about 65 GeV [6] even for light stops accessible at the current working Tevatron, this decay mode cannot be excluded. The decay $\tilde{t}_1 \rightarrow b\tilde{\chi}_1^+$ will obviously dominate over higher order decays if it is kinematically allowed.

In the case that this mode is kinematically forbidden, we have to consider higher order decays either at loop level or into more than two particles. There are two competitive modes for a stop accessible at LEP1.5/2 or the current Tevatron. One possibility is the flavor changing two body decay $\tilde{t}_1 \rightarrow c\tilde{\chi}_1^0$ occurring at one loop level. The other possibility is the four body decay into a b-quark, the LSP and two fermions. In [7] it has been shown, that for each choice of parameters the one loop decay will be the dominating one.

For the current working Tevatron both scenarios ($m_{\tilde{t}_1} > m_{\tilde{\chi}_1^+} + m_b$ or $m_{\tilde{t}_1} < m_{\tilde{\chi}_1^+} + m_b$) were considered in recent investigations [8]. Since for $m_{\tilde{t}_1} = m_t$ the cross section for the stop will be smaller by one order of magnitude than that for the top, $\sigma(\tilde{t}_1 \tilde{t}_1) \lesssim \frac{1}{10} \sigma(t\bar{t})$, this investigation for the current working Tevatron was done for stops lighter than 120 GeV. It was figured out, that in both cases the standard model background would be reducible by appropriate cuts and the stop signal should be distinguishable from comparable SM processes. Since the stop was not discovered by the Tevatron, new bounds on the masses of the lighter stop and on the LSP were found [9] assuming that the stop decays into a c quark and the LSP.

With the upgraded Tevatron, the LHC or a 500 GeV Linear Collider an enlarged stop mass range will be accessible. Due to the structure of the neutralino and chargino mass

matrices, $m_{\tilde{\chi}_1^+} \lesssim 2m_{\tilde{\chi}_1^0}$ holds. Therefore we can choose in the mass range beyond 160 GeV parameters, where $m_W + m_{\tilde{\chi}_1^0} + m_b < m_{\tilde{t}_1} < m_{\tilde{\chi}_1^+} + m_b$, leading to scenarios, where the three body decay $\tilde{t}_1 \rightarrow bW\tilde{\chi}_1^0$ is kinematically allowed but the two body decay $\tilde{t}_1 \rightarrow b\tilde{\chi}_1^+$ is still forbidden. The mass range $m_{\tilde{t}_1} > 160$ GeV will be accessible at the mentioned future colliders. It is, therefore, important to study how the rate for the three body decay compares to that for the flavour changing two body decay $\tilde{t}_1 \rightarrow c\tilde{\chi}_1^0$ [3].

In this paper we will study the physics of a stop, which is too heavy to be probed at colliders currently in operation but accessible for the upgraded Tevatron, the LHC or a 500 GeV Linear Collider in scenarios, where the two body decay into the b quark and the lighter chargino is forbidden. We will give a full analysis of the three body decay $\tilde{t}_1 \rightarrow bW\tilde{\chi}_1^0$ and will compare this decay with the flavor changing two body decay $\tilde{t}_1 \rightarrow c\tilde{\chi}_1^0$.

This paper is organized as follows. In Section 2 we give the analytical expressions for the invariant amplitudes of the decays considered here together with the respective parts of the Lagrangian of the MSSM. In Section 3 we discuss the total width of the three body decay for scenarios accessible either at an upgraded Tevatron, the LHC or at a 500 GeV Linear Collider and compare it with the flavor changing one. We conclude in Section 4 with some general remarks. The squared matrix element is given in the Appendix.

2 Analytical Calculation of the Widths

In this Section we will describe the analytical calculation of the decays considered in this paper. The explicit expressions for the squared amplitudes are listed in the Appendix.

We first describe briefly those parts of the MSSM, which we will use for our calculations following the notation of [4, 10]. The Feynman graphs for this process are shown in Fig. 1.

The neutralino sfermion fermion couplings and the chargino sfermion fermion couplings used here, we get from the respective parts of the Lagrangian,

$$\begin{aligned}\mathcal{L}_{f\tilde{f}\tilde{\chi}_i^0} &= g \sum_{k=1}^2 \left[\bar{f} \left(b_{ki}^f P_L + a_{ki}^f P_R \right) \tilde{\chi}_i^0 f_k + h.c. \right] \\ \mathcal{L}_{b\tilde{t}_1\tilde{\chi}_i^\pm} &= g\tilde{t}_1\bar{b} \left(l_{1i}^t P_R + k_{1i}^t P_L \right) \tilde{\chi}_i^\pm + h.c.\end{aligned}$$

The neutralino-chargino-W coupling entering in graph 2 we get from

$$\mathcal{L}_{W\tilde{\chi}_i^\pm\tilde{\chi}_j^0} = -gW_\mu^- \tilde{\chi}_i^- \left[\mathcal{O}_{ji}^L P_L + \mathcal{O}_{ji}^R P_R \right] \gamma^\mu \tilde{\chi}_j^0 + h.c.$$

where $P_{R,L} = \frac{1\pm\gamma_5}{2}$.

Finally we get the stop-sbottom-W coupling from

$$\mathcal{L}_{\tilde{t}_1\tilde{b}_jW} = \frac{-ig}{\sqrt{2}} \left\{ \cos\theta_b \cos\theta_t \tilde{b}_1^\dagger \overset{\leftrightarrow}{\partial}_\mu \tilde{t}_1 - \sin\theta_b \cos\theta_t \tilde{b}_2^\dagger \overset{\leftrightarrow}{\partial}_\mu \tilde{t}_1 \right\} W_\mu^+ + h.c.$$

The invariant amplitudes for the decay width ³ are given by

$$\mathcal{M}_{1,i=1,2} = -\frac{g^2}{\sqrt{2}} f_i(b) \cos\theta_t \frac{(p_{\tilde{t}} + p_{\tilde{b}_i})^\mu}{p_{\tilde{b}_i}^2 - m_{\tilde{b}_i}^2 - im_{\tilde{b}_i}\Gamma_{\tilde{b}_i}} \bar{u}(p_b) \left[b_{i1}^b P_L + a_{i1}^b P_R \right] v(p_{\tilde{\chi}_1^0}) \epsilon_\mu(p_W) \quad (7)$$

³For some subtleties concerning the fermion flow we refer to [11]

$$\mathcal{M}_{2,i=1,2} = g^2 \bar{u}(p_b) \left[l_{1i}^t P_R + k_{1i}^t P_L \right] \frac{\not{p}_{\tilde{\chi}_i^\pm} - m_{\tilde{\chi}_i^\pm}}{p_{\tilde{\chi}_i^\pm}^2 - m_{\tilde{\chi}_i^\pm}^2 - im_{\tilde{\chi}_i^\pm} \Gamma_{\tilde{\chi}_i^\pm}} \left[\mathcal{O}_{1i}^L P_L + \mathcal{O}_{1i}^R P_R \right] \gamma^\mu v(p_{\tilde{\chi}_1^0}) \epsilon_\mu(p_W) \quad (8)$$

$$\mathcal{M}_3 = -\frac{g^2}{\sqrt{2}} \bar{u}(p_b) \gamma^\mu \frac{1 - \gamma_5}{2} \frac{\not{p}_t + m_t}{p_t^2 - m_t^2 - im_t \Gamma_t} \left[b_{11}^t P_L + a_{11}^t P_R \right] v(p_{\tilde{\chi}_1^0}) \epsilon_\mu(p_W) \quad (9)$$

with $f_1(b) = \cos \theta_b$ and $f_2(b) = -\sin \theta_b$. The decay width is given by:

$$\Gamma(\tilde{t}_1 \rightarrow bW\tilde{\chi}_1^0) = \frac{1}{2m_{\tilde{t}_1} (2\pi)^5} \int \frac{d^3 p_b}{2E_b} \frac{d^3 p_W}{2E_W} \frac{d^3 p_{\tilde{\chi}_1^0}}{2E_{\tilde{\chi}_1^0}} \delta(p_{\tilde{t}_1} - p_b - p_W - p_{\tilde{\chi}_1^0}) |\mathcal{M}_1 + \mathcal{M}_2 + \mathcal{M}_3|^2 \quad (10)$$

with

$$\mathcal{M}_1 = \mathcal{M}_{1,1} + \mathcal{M}_{1,2}, \quad \mathcal{M}_2 = \mathcal{M}_{2,1} + \mathcal{M}_{2,2}. \quad (11)$$

In order to complete the picture we will also rewrite the results of [7] for the two body decay. They found, that the decay is dominated by top-charm squark mixing, which is induced at one loop level. In the limit $m_c \rightarrow 0$ only the left charm squark contributes to this mixing. The respective $\tilde{t}_1 - \tilde{t}_2 - \tilde{c}_L$ mixing is in the basis of (4) and in our notation given by

$$\mathcal{M}_{\tilde{t}_1 \tilde{t}_2 \tilde{c}_L}^2 = \begin{pmatrix} m_{\tilde{t}_1}^2 & 0 & \Delta_L \cos \theta_t + \Delta_R \sin \theta_t \\ 0 & m_{\tilde{t}_2}^2 & -\Delta_L \sin \theta_t + \Delta_R \cos \theta_t \\ \Delta_L^* \cos \theta_t + \Delta_R^* \sin \theta_t & -\Delta_L^* \sin \theta_t + \Delta_R^* \cos \theta_t & m_{\tilde{c}_L}^2 \end{pmatrix} \quad (12)$$

The Δ_L (Δ_R) are the mixing terms for the $\tilde{t}_L - \tilde{c}_L$ ($\tilde{t}_R - \tilde{c}_L$) mixings with

$$\Delta_L = -\frac{g^2}{16\pi^2} \ln \left(\frac{M_X^2}{m_W^2} \right) \frac{K_{tb}^* K_{cb} m_b^2}{2m_W^2 \cos^2 \beta} (M_Q^2 + M_D^2 + M_{H_1}^2 + |A_b|^2) \quad (13)$$

$$\Delta_R = \frac{g^2}{16\pi^2} \ln \left(\frac{M_X^2}{m_W^2} \right) \frac{K_{tb}^* K_{cb} m_b^2}{2m_W^2 \cos^2 \beta} m_t A_b^* \quad (14)$$

where M_X is a high scale which we assume to be the Planck mass to get a maximal mixing. The M_Q , M_D and M_{H_1} are the squark-, down-squark and Higgs mass terms and the K_{tb} and K_{cb} are the respective elements of the CKM matrix.

One gets eq. (13) and (14) as one step solutions in $\ln(M_P^2/M_W^2)$ of the renormalization group equation in the framework of supergravity theories. Note that one should stay away from $A_b = 0$ because otherwise higher order terms in $\ln(M_P^2/M_W^2)$ would become important for Δ_R . One should also note that in this approximation M_D , M_Q and M_{H_1} can be evaluated at any scale because the induced error would be of higher order. Therefore the expressions should be treated as rough estimations giving the order of magnitude for the mixing.

In the following ϵ gives the size of the charm squark component of the lighter stop, which we calculated numerically. Therefore in this decay mode the charm-squark component of the lighter stop couples with the charm quark and the LSP $\tilde{\chi}_1^0$ and the width is

given by

$$\Gamma(\tilde{t}_1 \rightarrow c\tilde{\chi}_1^0) = \frac{g^2}{16\pi}\epsilon^2|f_{11}^c|^2m_{\tilde{t}_1} \left(1 - \frac{m_{\tilde{\chi}_1^0}^2}{m_{\tilde{t}_1}^2}\right)^2 \quad (15)$$

where $f_{11}^c = -\frac{2\sqrt{2}}{3}\sin\theta_W N_{11} - \sqrt{2}(\frac{1}{2} - \frac{2}{3}\sin^2\theta_W)\frac{N_{12}}{\cos\theta_W}$.

3 Numerical Results

In this Section we will first describe that region of parameter space relevant for our calculations. Then we will discuss typical decay widths of the three body decay. In the last part we will compare these results for the three body decay with those for the one loop decay $\tilde{t}_1 \rightarrow c + \tilde{\chi}_1^0$.

Since the decay $\tilde{t}_1 \rightarrow W + b + \tilde{\chi}_1^0$ becomes of interest if $m_W + m_{\tilde{\chi}_1^0} + m_b < m_{\tilde{t}_1} < m_{\tilde{\chi}_1^+} + m_b$ we show in Fig. 2 different regions in the $M_2 - \mu$ plane where this relation is valid. We show results for two different values of $\tan\beta$ (2 and 30) and for stop masses of 170 GeV and 220 GeV. The lower stop mass is relevant for an upgraded Tevatron whereas the higher one is of interest for the LHC and a 500 GeV e^+e^- Linear Collider. Clearly for the LHC higher stop masses are also of interest. In such a case the region in the $M_2 - \mu$ plane will be shifted to higher values of M_2 and the M_2 range would become broader.

For fixing the parameters of the squark sector we have chosen the following procedure: additional to $\tan\beta$ and μ we have used within the stop sector $m_{\tilde{t}_1}$ and $\cos\theta_t$ as input parameters. For the sbottom sector we have fixed M_Q, M_D and A_b as input parameters. We have used this mixed set of parameters in order to avoid unnatural parameters in the sbottom sector. Note that because of $SU(2)$ invariance M_Q also appears in the stop mass matrix (eq. (2)). It can be seen by eq. (2), (3) and (4) that by variation of μ or $\tan\beta$ for fixed $m_{\tilde{t}_1}$ and $\cos\theta_t$ one also varies A_t and M_U . Therefore the mass of the heavier stop can be calculated from this set of input parameters:

$$m_{\tilde{t}_2}^2 = \frac{2M_Q^2 + 2m_Z^2 \cos 2\beta (\frac{1}{2} - \frac{2}{3}\sin^2\theta_W) + 2m_t^2 - m_{\tilde{t}_1}^2 (1 + \cos 2\theta_t)}{1 - \cos 2\theta_t} \quad (16)$$

In the sbottom sector obviously the physical quantities $m_{\tilde{b}_i}$ and $\cos\theta_b$ changes with μ and $\tan\beta$.

3.1 The Three Body Decay

We shall now discuss the numerical results for the decay width $\Gamma(\tilde{t}_1 \rightarrow W + b + \tilde{\chi}_1^0)$. The results relevant for $m_{\tilde{t}_1} = 220$ GeV, relevant for the Linear Collider and the LHC, are shown in Fig. 3 and for $m_{\tilde{t}_1} = 170$ GeV, relevant for an upgraded Tevatron, in Fig. 4. For the other physical quantities we used $m_W = 80$ GeV, $\sin^2\theta_W = 0.23$, $m_b = 5$ GeV and $m_t = 175$ GeV.

First we shall focus on the case 220 GeV. As can be seen from Fig. 2 M_2 can vary between ~ 210 GeV and ~ 270 GeV. Within this small region there is no significant change of the nature of the LSP and the charginos for the allowed values of μ . Therefore we have fixed M_2 at 250 GeV. We have also found that our results depend only weakly on

the parameters of the sbottom sector. To be specific we have used $M_Q = M_D = 500$ GeV and $A_b = -350$ GeV. We have checked that with these choices of parameters the following relations hold: $m_{\tilde{b}_1} + m_W > m_{\tilde{t}_1}$ and $m_{\tilde{b}_2}, m_{\tilde{t}_2} < 1$ TeV.

In Fig. 3a we show the dependence of the decay width on $\tan\beta$ for $\cos\theta_t = 0.7$, $\mu = \pm 500$ GeV and $\mu = \pm 750$ GeV. One can see that the decay width varies between 0.18 and 1.65 KeV. For negative μ we have a maximum at $\tan\beta \sim 20$ due to the positive interference between the top (\mathcal{M}_3) and chargino terms ($\mathcal{M}_{2,i}$). For small $\tan\beta$ and positive μ the behaviour is dominated by the fact that the lighter chargino is nearly on mass shell. To control this effect we have taken into account the decay widths in all propagators.

In Fig. 3b we show the dependence of the decay width on $\cos\theta_t$ for $\tan\beta = 20$, $\mu = \pm 500$ GeV and $\mu = \pm 750$. As one can see the decay widths varies between 10 eV and 0.78 KeV. The maximum near $\cos\theta = 0.25$ is due to the interference of the gaugino and higgsino parts in the squark couplings. One can see that the decay width is slightly higher for positive μ which results from different kinematics.

The now following discussion for the case $m_{\tilde{t}_1} = 170$ GeV will be changed slightly. From Fig. 2 one can see that the region in $M_2 - \mu$ plane is smaller compared to the case above and varies with $\tan\beta$. Therefore we show only the dependence on $\cos\theta_t$. We show this for four different choices of M_2, μ and $\tan\beta$ (see Table 1) in Fig. 4. For the sbottom sector we have again taken $M_Q = M_D = 500$ GeV and $A_b = -350$ GeV.

The qualitative behaviour of this dependence is similar to that for $m_{\tilde{t}_1} = 220$ GeV. We also reach a maximum for the width for $0 < \cos\theta_t < 0.25$ by the same reason already mentioned for the case $m_{\tilde{t}_1} = 220$ GeV. But the width is in this case even smaller, a few eV or even below. This small width arises by the small difference of the masses $\Delta m = m_{\tilde{t}_1} - m_b - m_W - m_{\tilde{\chi}_1^0}$. For our choice of parameters, Δm varies between 0.6 GeV (scenario a) and 2.4 GeV (scenario c).

3.2 The Comparison of the Decay Modes

We now will compare our results for the decay $\tilde{t}_1 \rightarrow bW\tilde{\chi}_1^0$ with those of the decay $\tilde{t}_1 \rightarrow c\tilde{\chi}_1^0$. The latter was calculated in [7]. As already stated in Section 2 the used formula for the two body decay gives a rough estimation for the order of magnitude. Therefore we will mainly demonstrate the existence of parameter regions where one of the decays clearly dominates.

Here we will follow the same procedure as in the last Section. Before discussing our results in detail we will give some general remarks. The crucial parameter for the width $\Gamma(\tilde{t}_1 \rightarrow c\tilde{\chi}_1^0)$ is the size of the charm squark component ϵ of the physical stop. We reached in some scenarios values for ϵ bigger than 0.1. ϵ will become big if (i) $m_{\tilde{t}_1}$ and $m_{\tilde{c}_L}$ have almost the same size, (ii) $\tan\beta$ becomes big ($\cos\beta$ small) which will enhance Δ_L and Δ_R (iii) $\tan\theta_t \sim \Delta_L/\Delta_R$ which will maximize the \mathcal{M}_{13}^2 and \mathcal{M}_{31}^2 components of the mixing matrix $\mathcal{M}_{\tilde{t}_1\tilde{t}_2\tilde{c}_L}^2$ (eq. (12)) and (iv) the parameters M_D, M_Q, M_{H_1} and A_b entering Δ_L and Δ_R are big.

The charm squark mass is given by the value of M_Q and the contribution of the D-term and is with our choice of parameters significantly higher than the stop mass ($m_{\tilde{c}_L} = 498.3$ GeV (497.1 GeV) for $\tan\beta = 2(30)$ respectively). Therefore we do not have an effect from the charm squark mass which could enhance the width of the two body

decay as mentioned above.

From Fig. 2 one can see that in the allowed regions M_2 is smaller than μ in most of the cases. Therefore the lightest neutralino and the lighter chargino will be mainly gaugino-like. Due to this fact the influence of μ is mainly through phase space effects. In the case that $\mu \leq M_2$ the coupling $\tilde{\chi}_1^0 \tilde{c} c$ will be small leading to an increase of the branching ratio of the three body decay.

In Fig. 5 we consider the case $m_{\tilde{t}_1} = 220$ GeV. As a typical example we take the case $\mu = -500$ GeV from Fig. 3 where we show the corresponding decay width of the three body decay. Fig. 5a shows the branching ratios as a function of $\tan \beta$ for $\cos \theta_t = 0.7$. The reason for the dominance of the two body decay for large $\tan \beta$ is the above mentioned dependence of $\Delta_{L,R}$ on $1/\cos \beta$. Therefore the branching ratio for the three body decay is below 1% for $\tan \beta > 30$. In Fig. 5b we show the branching ratio as function of $\cos \theta_t$ for $\tan \beta = 20$. As already mentioned, ϵ will be maximized if $\tan \theta_t \sim \Delta_L/\Delta_R$, which happens with our choice of A_b if $\cos \theta_t$ and $\sin \theta_t$ have the opposite sign and $|\cos \theta_t|$ is big. As we can see this results in a strong dominance of the two body decay for $\cos \theta_t < -0.4 (> 0.7)$ whereas the three body decay is dominating near $\cos \theta_t = 0$.

The case $m_{\tilde{t}_1} = 170$ GeV is shown in Fig. 6 (the parameters are given in Table 1), where we see a similar feature. The decay $\tilde{t}_1 \rightarrow c\tilde{\chi}_1^0$ becomes dominant (or at least important in case of $\mu = -1000$ GeV and $\tan \beta = 2$) if $|\cos \theta_t|$ becomes big. The dominance is stronger for $\tan \beta = 30$ than for $\tan \beta = 2$ as already explained. It is worthwhile to mention that even for $\tan \beta = 30$ for very small $\cos \theta_t$ the three body decay may dominate resulting in this remarkable peak for the respective branching fractions.

As main result we conclude, that there exists parameter regions where either the three body decay or the two body decay dominates clearly. This dominance may become so strong, that the mentioned uncertainty is of no relevance in the respective parameter region. Another important result is that we never got total decay widths for the light stop bigger than 100 KeV. Therefore in all considered cases the lifetime of the light stop will be larger than the hadronization scale.

4 Conclusion

We calculated the three body decay $\tilde{t}_1 \rightarrow bW\tilde{\chi}_1^0$ and compared these results with those for the two body decay $\tilde{t}_1 \rightarrow c\tilde{\chi}_1^0$ [7]. These both decays will be the competitive ones in that part of the parameter space accessible for either the upgraded Tevatron, the LHC or a 500 GeV Linear Collider, where the two body tree level decay $\tilde{t}_1 \rightarrow b\tilde{\chi}_1^\pm$ is kinematically forbidden.

We found that the branching ratios are very sensitive to the choice of the free parameters of the model. Especially the stop mixing angle θ_t , the difference between the masses of the lighter stop $m_{\tilde{t}_1}$ and the lefthanded charm squark $m_{\tilde{c}_L}$ and the value of $\tan \beta$ are crucial parameters, whereas M_2 and μ are mainly important in order to specify the relevant regions of the parameter space. Depending on the specific values of these parameters each decay mode may become the dominant one and none of them should be neglected.

In case of a dominance of the three body decay, stop production leads to the signature

$2b+2W+\cancel{E}$ which will result in the final signature $(2-4)jets+(0-2)charged\ leptons+\cancel{E}$. It is not trivial to answer the question, if a stop in this parameter region is distinguishable from a top quark. Further investigations especially of the differential widths including Monte Carlo simulations are needed to solve this problem.

Another important problem is that of hadronization of the produced stops. We calculated a width in the range between 10 eV and 100 KeV. One can clearly see that the lifetime of the light stop is bigger than the hadronization time. Therefore the mentioned Monte Carlo studies have also to address all problems related to hadronization.

We have shown, that the three body decay $\tilde{t}_1 \rightarrow bW\tilde{\chi}_1^0$ is of major interest for stop physics at the upgraded Tevatron as well as a 500 GeV Linear Collider and the LHC. This decay cannot be neglected in future investigations. But we also have shown that further investigations are needed in order to give realistic predictions for experiments at future colliders.

Acknowledgements

We would like to thank X. Tata, A. Bartl and W. Majerotto for many helpful discussions. T.W. also is gratefully to the Departement of Physics and Astronomy of the University of Hawaii at Manoa, the Departement of Physics and Astronomy of the University of Wisconsin at Madison and the Institut für Theoretische Physik der Universität Wien, where part of this work was done, for the kind hospitality and the pleasant atmosphere. T.W. is supported by the Deutsche Forschungsgemeinschaft (DFG), and W.P. by the ‘‘Fonds zur Förderung der wissenschaftlichen Forschung’’ of Austria, project no. P10843-PHY.

Appendix

In this Appendix we give the full expressions of the squared amplitudes $|\sum_n \mathcal{M}_n|^2$, with $\mathcal{M}_1 := \mathcal{M}_{1,1} + \mathcal{M}_{1,2}$ and $\mathcal{M}_2 := \mathcal{M}_{2,1} + \mathcal{M}_{2,2}$, in terms of four-vector products $p_l \cdot p_k$ of the outer momenta of the bottom quark p_b , the W -boson p_W and the lightest Neutralino $p_{\tilde{\chi}_1^0}$. All sums run over $i, j = 1, 2$. The momenta of the virtual particles are given by $p_{\tilde{b}_i} = p_{\tilde{b}_j} = p_b + p_{\tilde{\chi}_1^0}$, $p_{\tilde{\chi}_i^\pm} = p_{\tilde{\chi}_j^\pm} = p_W + p_{\tilde{\chi}_1^0}$ and $p_t = p_W + p_b$. In this notation the squared amplitudes are given by

$$\begin{aligned}
|\mathcal{M}_1|^2 &= 16 \sum_{i,j} a_{11}^{i*} a_{11}^j \frac{1}{(p_{\tilde{b}_i}^2 - m_{\tilde{b}_i}^2 + im_{\tilde{b}_i} \Gamma_{\tilde{b}_i})} \frac{1}{(p_{\tilde{b}_j}^2 - m_{\tilde{b}_j}^2 - im_{\tilde{b}_j} \Gamma_{\tilde{b}_j})} \\
&\quad \left\{ \left[\frac{1}{m_W^2} \left((p_b \cdot p_W)^2 + (p_{\tilde{\chi}_1^0} \cdot p_W)^2 + 2p_b \cdot p_W p_{\tilde{\chi}_1^0} \cdot p_W \right) - m_b^2 - m_{\tilde{\chi}_1^0}^2 - 2p_b \cdot p_{\tilde{\chi}_1^0} \right] \times \right. \\
&\quad \left. \left[(a_{12}^{i*} a_{12}^j + b_{12}^{i*} b_{12}^j) p_b \cdot p_{\tilde{\chi}_1^0} - (a_{12}^{i*} a_{12}^j - b_{12}^{i*} b_{12}^j) m_b m_{\tilde{\chi}_1^0} \right] \right\} \quad (17) \\
|\mathcal{M}_2|^2 &= \sum_{i,j} \frac{1}{(p_{\tilde{\chi}_i^\pm}^2 - m_{\tilde{\chi}_i^\pm}^2 + im_{\tilde{\chi}_i^\pm} \Gamma_{\tilde{\chi}_i^\pm})} \frac{1}{(p_{\tilde{\chi}_j^\pm}^2 - m_{\tilde{\chi}_j^\pm}^2 - im_{\tilde{\chi}_j^\pm} \Gamma_{\tilde{\chi}_j^\pm})} \\
&\quad 4(a_{21}^{i*} a_{22}^{i*} a_{21}^j a_{22}^j + b_{21}^{i*} b_{22}^{i*} b_{21}^j b_{22}^j + a_{21}^{i*} a_{22}^{i*} b_{21}^j b_{22}^j + a_{21}^{i*} a_{22}^j b_{21}^j b_{22}^{i*} +
\end{aligned}$$

$$\begin{aligned}
& a_{21}^{i*} a_{21}^j b_{22}^{i*} b_{22}^j + b_{21}^{i*} b_{22}^{i*} a_{21}^j a_{22}^j + b_{21}^{i*} b_{22}^j a_{21}^j a_{22}^{i*} + b_{21}^{i*} b_{21}^j a_{22}^{i*} a_{22}^j \\
& \left[p_b \cdot p_{\tilde{\chi}_1^0} (m_{\tilde{\chi}_1^0}^2 - m_W^2) + 4p_{\tilde{\chi}_1^0} \cdot p_W (p_b \cdot p_W + p_b \cdot p_{\tilde{\chi}_1^0}) + \right. \\
& \left. 2m_{\tilde{\chi}_1^0}^2 (2p_b \cdot p_W + m_{\tilde{\chi}_1^0}^2) + \frac{2}{m_W^2} p_{\tilde{\chi}_1^0} \cdot p_W (2p_b \cdot p_{\tilde{\chi}_1^0} p_W \cdot p_{\tilde{\chi}_1^0} - p_b \cdot p_W m_{\tilde{\chi}_1^0}^2) \right] \\
& + 12(a_{21}^{i*} a_{22}^{i*} a_{21}^j a_{22}^j + b_{21}^{i*} b_{22}^{i*} b_{21}^j b_{22}^j - a_{21}^{i*} a_{22}^{i*} b_{21}^j b_{22}^j + a_{21}^{i*} a_{22}^j b_{21}^j b_{22}^{i*} - \\
& a_{21}^{i*} a_{21}^j b_{22}^{i*} b_{22}^j - b_{21}^{i*} b_{22}^{i*} a_{21}^j a_{22}^j + b_{21}^{i*} b_{22}^j a_{21}^j a_{22}^{i*} - b_{21}^{i*} b_{21}^j a_{22}^{i*} a_{22}^j) \\
& m_{\tilde{\chi}_1^0} m_b m_{\tilde{\chi}_i^\pm} m_{\tilde{\chi}_j^\pm} \\
& - 12 \left(m_{\tilde{\chi}_j^\pm} (a_{21}^{i*} a_{22}^{i*} a_{21}^j a_{22}^j - b_{21}^{i*} b_{22}^{i*} b_{21}^j b_{22}^j - a_{21}^{i*} a_{22}^{i*} b_{21}^j b_{22}^j + a_{21}^{i*} a_{22}^j b_{21}^j b_{22}^{i*} - \right. \\
& a_{21}^{i*} a_{21}^j b_{22}^{i*} b_{22}^j + b_{21}^{i*} b_{22}^{i*} a_{21}^j a_{22}^j - b_{21}^{i*} b_{22}^j a_{21}^j a_{22}^{i*} + b_{21}^{i*} b_{21}^j a_{22}^{i*} a_{22}^j) + i \leftrightarrow j) \\
& m_{\tilde{\chi}_1^0} (p_b \cdot p_{\tilde{\chi}_1^0} + p_b \cdot p_W) \\
& + (a_{21}^{i*} a_{22}^{i*} a_{21}^j a_{22}^j + b_{21}^{i*} b_{22}^{i*} b_{21}^j b_{22}^j - a_{21}^{i*} a_{22}^{i*} b_{21}^j b_{22}^j - a_{21}^{i*} a_{22}^j b_{21}^j b_{22}^{i*} + \\
& a_{21}^{i*} a_{21}^j b_{22}^{i*} b_{22}^j - b_{21}^{i*} b_{22}^{i*} a_{21}^j a_{22}^j - b_{21}^{i*} b_{22}^j a_{21}^j a_{22}^{i*} + b_{21}^{i*} b_{21}^j a_{22}^{i*} a_{22}^j) \\
& m_{\tilde{\chi}_i^\pm} m_{\tilde{\chi}_j^\pm} \left(\frac{8}{m_W^2} p_{\tilde{\chi}_1^0} \cdot p_W p_b \cdot p_W + 4p_{\tilde{\chi}_1^0} \cdot p_b \right) \\
& + 12(a_{21}^{i*} a_{22}^{i*} a_{21}^j a_{22}^j + b_{21}^{i*} b_{22}^{i*} b_{21}^j b_{22}^j + a_{21}^{i*} a_{22}^{i*} b_{21}^j b_{22}^j - a_{21}^{i*} a_{22}^j b_{21}^j b_{22}^{i*} - \\
& a_{21}^{i*} a_{21}^j b_{22}^{i*} b_{22}^j + b_{21}^{i*} b_{22}^{i*} a_{21}^j a_{22}^j - b_{21}^{i*} b_{22}^j a_{21}^j a_{22}^{i*} - b_{21}^{i*} b_{21}^j a_{22}^{i*} a_{22}^j) \\
& m_{\tilde{\chi}_1^0} m_b (m_W^2 + m_{\tilde{\chi}_1^0}^2 + 2p_{\tilde{\chi}_1^0} \cdot p_W) \\
& - \left(m_{\tilde{\chi}_j^\pm} (a_{21}^{i*} a_{22}^{i*} a_{21}^j a_{22}^j - b_{21}^{i*} b_{22}^{i*} b_{21}^j b_{22}^j - a_{21}^{i*} a_{22}^{i*} b_{21}^j b_{22}^j - a_{21}^{i*} a_{22}^j b_{21}^j b_{22}^{i*} + \right. \\
& a_{21}^{i*} a_{21}^j b_{22}^{i*} b_{22}^j + b_{21}^{i*} b_{22}^{i*} a_{21}^j a_{22}^j + b_{21}^{i*} b_{22}^j a_{21}^j a_{22}^{i*} - b_{21}^{i*} b_{21}^j a_{22}^{i*} a_{22}^j) + i \leftrightarrow j) \\
& m_b \left(12p_{\tilde{\chi}_1^0} \cdot p_W + \frac{8}{m_W^2} (p_{\tilde{\chi}_1^0} \cdot p_W)^2 + 4m_{\tilde{\chi}_1^0}^2 \right) \tag{18}
\end{aligned}$$

$$\begin{aligned}
|\mathcal{M}_3|^2 &= \frac{1}{|p_t^2 - m_t^2 - im_t \Gamma_t|^2} \left\{ 8|a_{32}|^2 |a_{31} + b_{31}|^2 \right. \\
& \left[m_b^2 (-6p_W \cdot p_{\tilde{\chi}_1^0} - 3p_b \cdot p_{\tilde{\chi}_1^0}) + \frac{4}{m_W^2} p_{\tilde{\chi}_1^0} \cdot p_W (p_b \cdot p_W)^2 - \right. \\
& \left. \frac{2}{m_W^2} m_b^2 p_{\tilde{\chi}_1^0} \cdot p_b p_W \cdot p_b + 3m_W^2 p_{\tilde{\chi}_1^0} \cdot p_b + 4p_b \cdot p_W (p_{\tilde{\chi}_1^0} \cdot p_b - p_{\tilde{\chi}_1^0} \cdot p_W) \right] \\
& + 8m_t^2 |a_{32}|^2 |a_{31} - b_{31}|^2 \left(\frac{2}{m_W^2} p_{\tilde{\chi}_1^0} \cdot p_W p_b \cdot p_W + p_{\tilde{\chi}_1^0} \cdot p_b \right) \\
& \left. - 16m_t m_{\tilde{\chi}_1^0} (|a_{31}|^2 - |b_{31}|^2) |a_{32}|^2 \left(3p_b \cdot p_W + \frac{2}{m_W^2} (p_b \cdot p_W)^2 - m_b^2 \right) \right\} \tag{19}
\end{aligned}$$

$$\begin{aligned}
2\text{Re}(\mathcal{M}_1 \mathcal{M}_2^*) &= 8\text{Re} \sum_{i,j} a_{11}^j \frac{1}{(p_{\tilde{\chi}_i^\pm}^2 - m_{\tilde{\chi}_i^\pm}^2 + im_{\tilde{\chi}_i^\pm} \Gamma_{\tilde{\chi}_i^\pm})} \frac{1}{(p_{\tilde{b}_j}^2 - m_{\tilde{b}_j}^2 - im_{\tilde{b}_j} \Gamma_{\tilde{b}_j})} \\
& \left\{ (a_{21}^{i*} a_{22}^{i*} a_{12}^j + a_{21}^{i*} b_{22}^{i*} b_{12}^j + a_{22}^{i*} b_{21}^{i*} b_{12}^j + b_{21}^{i*} b_{22}^{i*} a_{12}^j) \right.
\end{aligned}$$

$$\begin{aligned}
& \left[\frac{m_{\tilde{\chi}_1^0}^2}{m_W^2} (2(p_b \cdot p_W)^2 + 2p_{\tilde{\chi}_1^0} \cdot p_W p_b \cdot p_W) - \frac{2}{m_W^2} p_{\tilde{\chi}_1^0} \cdot p_b (2(p_{\tilde{\chi}_1^0} \cdot p_W)^2 + \right. \\
& 2p_{\tilde{\chi}_1^0} \cdot p_W p_b \cdot p_W) - 2m_b^2 (m_{\tilde{\chi}_1^0}^2 + p_W \cdot p_b) - 2p_b \cdot p_{\tilde{\chi}_1^0} p_W \cdot p_{\tilde{\chi}_1^0} + \\
& 2m_{\tilde{\chi}_1^0}^2 (p_{\tilde{\chi}_1^0} \cdot p_b + p_W \cdot p_b) + 2p_{\tilde{\chi}_1^0} \cdot p_b p_W \cdot p_b + 4(p_b \cdot p_{\tilde{\chi}_1^0})^2 \left. \right] \\
& - m_{\tilde{\chi}_1^0} m_{\tilde{\chi}_i^\pm} (a_{21}^{i*} a_{22}^{i*} a_{12}^j - a_{21}^{i*} b_{22}^{i*} b_{12}^j + a_{22}^{i*} b_{21}^{i*} b_{12}^j - b_{21}^{i*} b_{22}^{i*} a_{12}^j) \\
& \left[\frac{1}{m_W^2} (2(p_b \cdot p_W)^2 + 2p_{\tilde{\chi}_1^0} \cdot p_W p_b \cdot p_W) - 2m_b^2 - 2p_b \cdot p_{\tilde{\chi}_1^0} \right] \\
& + [m_b m_{\tilde{\chi}_1^0} (a_{21}^{i*} a_{22}^{i*} a_{12}^j - a_{21}^{i*} b_{22}^{i*} b_{12}^j - a_{22}^{i*} b_{21}^{i*} b_{12}^j + b_{21}^{i*} b_{22}^{i*} a_{12}^j) \\
& + m_b m_{\tilde{\chi}_i^\pm} (a_{21}^{i*} a_{22}^{i*} a_{12}^j + a_{21}^{i*} b_{22}^{i*} b_{12}^j - a_{22}^{i*} b_{21}^{i*} b_{12}^j - b_{21}^{i*} b_{22}^{i*} a_{12}^j)] \\
& \left. \left[\frac{1}{m_W^2} (2(p_{\tilde{\chi}_1^0} \cdot p_W)^2 + 2p_{\tilde{\chi}_1^0} \cdot p_W p_b \cdot p_W) - 2m_{\tilde{\chi}_1^0}^2 - 2p_b \cdot p_{\tilde{\chi}_1^0} \right] \right\} \quad (20)
\end{aligned}$$

$$\begin{aligned}
2\text{Re}(\mathcal{M}_1^* \mathcal{M}_3) &= 8\text{Re} \sum_i a_{32} a_{11}^{i*} \frac{1}{(p_t^2 - m_t^2 - im_t \Gamma_t)} \frac{1}{(p_{b_i}^2 - m_{b_i}^2 + im_{b_i} \Gamma_{b_i})} \\
& \left\{ (a_{31} a_{12}^{i*} + b_{31} b_{12}^{i*} + a_{12}^{i*} b_{31} + a_{31} b_{12}^{i*}) \right. \\
& \left[-\frac{m_b^2}{m_W^2} (2(p_{\tilde{\chi}_1^0} \cdot p_W)^2 + 2p_{\tilde{\chi}_1^0} \cdot p_W p_b \cdot p_W) + \frac{2}{m_W^2} p_{\tilde{\chi}_1^0} \cdot p_b (2(p_b \cdot p_W)^2 + \right. \\
& 2p_{\tilde{\chi}_1^0} \cdot p_W p_b \cdot p_W) + 2m_{\tilde{\chi}_1^0}^2 (m_b^2 + p_W \cdot p_b) + 2p_b \cdot p_{\tilde{\chi}_1^0} p_W \cdot p_b - \\
& 2m_b^2 (p_{\tilde{\chi}_1^0} \cdot p_W + p_{\tilde{\chi}_1^0} \cdot p_b) - 2p_{\tilde{\chi}_1^0} \cdot p_b p_W \cdot p_{\tilde{\chi}_1^0} - 4(p_b \cdot p_{\tilde{\chi}_1^0})^2 \left. \right] \\
& + m_b m_t (a_{31} a_{12}^{i*} + b_{31} b_{12}^{i*} - a_{12}^{i*} b_{31} - a_{31} b_{12}^{i*}) \\
& \left[\frac{1}{m_W^2} (2(p_{\tilde{\chi}_1^0} \cdot p_W)^2 + 2p_{\tilde{\chi}_1^0} \cdot p_W p_b \cdot p_W) - 2m_{\tilde{\chi}_1^0}^2 - 2p_b \cdot p_{\tilde{\chi}_1^0} \right] \\
& - [m_t m_{\tilde{\chi}_1^0} (a_{31} a_{12}^{i*} - b_{31} b_{12}^{i*} - a_{12}^{i*} b_{31} + a_{31} b_{12}^{i*}) \\
& + m_b m_{\tilde{\chi}_1^0} (a_{31} a_{12}^{i*} - b_{31} b_{12}^{i*} + a_{12}^{i*} b_{31} - a_{31} b_{12}^{i*})] \\
& \left. \left[\frac{1}{m_W^2} (2(p_b \cdot p_W)^2 + 2p_{\tilde{\chi}_1^0} \cdot p_W p_b \cdot p_W) - 2m_b^2 - 2p_b \cdot p_{\tilde{\chi}_1^0} \right] \right\} \quad (21)
\end{aligned}$$

$$\begin{aligned}
2\text{Re}(\mathcal{M}_2^* \mathcal{M}_3) &= 8\text{Re} \sum_i a_{32} \frac{1}{(p_t^2 - m_t^2 - im_t \Gamma_t)} \frac{1}{(p_{\tilde{\chi}_i^\pm}^2 - m_{\tilde{\chi}_i^\pm}^2 + im_{\tilde{\chi}_i^\pm} \Gamma_{\tilde{\chi}_i^\pm})} \\
& \left\{ (a_{21}^{i*} a_{22}^{i*} a_{31} + b_{21}^{i*} a_{22}^{i*} a_{31} + a_{21}^{i*} b_{22}^{i*} b_{31} + b_{21}^{i*} b_{22}^{i*} b_{31}) \right. \\
& + a_{21}^{i*} b_{22}^{i*} a_{31} + b_{21}^{i*} b_{22}^{i*} a_{31} + a_{21}^{i*} a_{22}^{i*} b_{31} + b_{21}^{i*} a_{22}^{i*} b_{31}) \\
& \left[2\frac{m_b^2}{m_W^2} (p_{\tilde{\chi}_1^0} \cdot p_W)^2 - m_{\tilde{\chi}_1^0}^2 m_b^2 - p_{\tilde{\chi}_1^0} \cdot p_b m_W^2 - \right. \\
& \frac{2}{m_W^2} p_b \cdot p_W (2p_{\tilde{\chi}_1^0} \cdot p_b p_{\tilde{\chi}_1^0} \cdot p_W - p_b \cdot p_W m_{\tilde{\chi}_1^0}^2) \\
& + 2p_b \cdot p_{\tilde{\chi}_1^0} p_W \cdot p_{\tilde{\chi}_1^0} + p_b \cdot p_W m_{\tilde{\chi}_1^0}^2 + 2p_b \cdot p_W p_b \cdot p_{\tilde{\chi}_1^0} + \\
& \left. p_{\tilde{\chi}_1^0} \cdot p_W m_b^2 + 4(p_{\tilde{\chi}_1^0} \cdot p_b)^2 + 4p_b \cdot p_W p_{\tilde{\chi}_1^0} \cdot p_W \right]
\end{aligned}$$

$$\begin{aligned}
& +m_{\tilde{\chi}_i^\pm} m_t (a_{21}^{i*} a_{22}^{i*} a_{31} + b_{21}^{i*} a_{22}^{i*} a_{31} + a_{21}^{i*} b_{22}^{i*} b_{31} + b_{21}^{i*} b_{22}^{i*} b_{31} \\
& - a_{21}^{i*} b_{22}^{i*} a_{31} - b_{21}^{i*} a_{22}^{i*} a_{31} - a_{21}^{i*} a_{22}^{i*} b_{31} - b_{21}^{i*} a_{22}^{i*} b_{31}) \\
& \left(\frac{2}{m_W^2} p_b \cdot p_W p_{\tilde{\chi}_1^0} \cdot p_W + p_b \cdot p_{\tilde{\chi}_1^0} \right) \\
& - 3m_{\tilde{\chi}_1^0} m_t (a_{21}^{i*} a_{22}^{i*} a_{31} + b_{21}^{i*} a_{22}^{i*} a_{31} - a_{21}^{i*} b_{22}^{i*} b_{31} - b_{21}^{i*} b_{22}^{i*} b_{31} \\
& + a_{21}^{i*} b_{22}^{i*} a_{31} + b_{21}^{i*} a_{22}^{i*} a_{31} - a_{21}^{i*} a_{22}^{i*} b_{31} - b_{21}^{i*} a_{22}^{i*} b_{31}) \\
& (p_b \cdot p_{\tilde{\chi}_1^0} + p_b \cdot p_W) \\
& - m_{\tilde{\chi}_1^0} m_{\tilde{\chi}_i^\pm} (a_{21}^{i*} a_{22}^{i*} a_{31} + b_{21}^{i*} a_{22}^{i*} a_{31} - a_{21}^{i*} b_{22}^{i*} b_{31} - b_{21}^{i*} b_{22}^{i*} b_{31} \\
& - a_{21}^{i*} b_{22}^{i*} a_{31} - b_{21}^{i*} a_{22}^{i*} a_{31} + a_{21}^{i*} a_{22}^{i*} b_{31} + b_{21}^{i*} a_{22}^{i*} b_{31}) \\
& \left(\frac{2}{m_W^2} (p_b \cdot p_W)^2 + m_b^2 + 3p_b \cdot p_W \right) \\
& - m_b m_t (a_{21}^{i*} a_{22}^{i*} a_{31} - b_{21}^{i*} a_{22}^{i*} a_{31} + a_{21}^{i*} b_{22}^{i*} b_{31} - b_{21}^{i*} b_{22}^{i*} b_{31} \\
& - a_{21}^{i*} b_{22}^{i*} a_{31} + b_{21}^{i*} a_{22}^{i*} a_{31} - a_{21}^{i*} a_{22}^{i*} b_{31} + b_{21}^{i*} a_{22}^{i*} b_{31}) \\
& \left(\frac{2}{m_W^2} (p_{\tilde{\chi}_1^0} \cdot p_W)^2 + m_{\tilde{\chi}_1^0}^2 + 3p_{\tilde{\chi}_1^0} \cdot p_W \right) \\
& - 3m_{\tilde{\chi}_i^\pm} m_b (a_{21}^{i*} a_{22}^{i*} a_{31} - b_{21}^{i*} a_{22}^{i*} a_{31} + a_{21}^{i*} b_{22}^{i*} b_{31} - b_{21}^{i*} b_{22}^{i*} b_{31} \\
& + a_{21}^{i*} b_{22}^{i*} a_{31} - b_{21}^{i*} a_{22}^{i*} a_{31} + a_{21}^{i*} a_{22}^{i*} b_{31} - b_{21}^{i*} a_{22}^{i*} b_{31}) \\
& (p_{\tilde{\chi}_1^0} \cdot p_b + p_{\tilde{\chi}_1^0} \cdot p_W) \\
& + m_b m_{\tilde{\chi}_1^0} (a_{21}^{i*} a_{22}^{i*} a_{31} - b_{21}^{i*} a_{22}^{i*} a_{31} - a_{21}^{i*} b_{22}^{i*} b_{31} + b_{21}^{i*} b_{22}^{i*} b_{31} \\
& - a_{21}^{i*} b_{22}^{i*} a_{31} + b_{21}^{i*} a_{22}^{i*} a_{31} + a_{21}^{i*} a_{22}^{i*} b_{31} - b_{21}^{i*} a_{22}^{i*} b_{31}) \\
& \left(3m_W^2 + 3p_{\tilde{\chi}_1^0} \cdot p_W + 3p_b \cdot p_W + p_{\tilde{\chi}_1^0} \cdot p_b + \frac{2}{m_W^2} p_{\tilde{\chi}_1^0} \cdot p_W p_b \cdot p_W \right) \\
& + 3m_{\tilde{\chi}_i^\pm} m_b m_{\tilde{\chi}_1^0} m_t (a_{21}^{i*} a_{22}^{i*} a_{31} - b_{21}^{i*} a_{22}^{i*} a_{31} - a_{21}^{i*} b_{22}^{i*} b_{31} + b_{21}^{i*} b_{22}^{i*} b_{31} \\
& + a_{21}^{i*} b_{22}^{i*} a_{31} - b_{21}^{i*} a_{22}^{i*} a_{31} - a_{21}^{i*} a_{22}^{i*} b_{31} + b_{21}^{i*} a_{22}^{i*} b_{31}) \} \tag{22}
\end{aligned}$$

Here the a_{nm}^k and b_{nm}^k are coupling constants and given by [10]:

$$\begin{aligned}
a_{11}^1 &= -\frac{g}{\sqrt{2}} \cos \theta_b \cos \theta_t \\
a_{11}^2 &= \frac{g}{\sqrt{2}} \sin \theta_b \cos \theta_t \\
a_{12}^i &= \frac{g}{2} (a_{i1}^b + b_{i1}^b), & b_{12}^i &= \frac{g}{2} (a_{i1}^b - b_{i1}^b) \\
a_{21}^i &= \frac{g}{2} (l_{1i}^t + k_{1i}^t), & b_{21}^i &= \frac{g}{2} (l_{1i}^t - k_{1i}^t) \\
a_{22}^i &= -\frac{g}{2} (\mathcal{O}_{1i}^L + \mathcal{O}_{1i}^R), & b_{22}^i &= -\frac{g}{2} (\mathcal{O}_{1i}^L - \mathcal{O}_{1i}^R) \\
a_{31} &= \frac{g}{2} (a_{11}^t + b_{11}^t), & b_{31} &= \frac{g}{2} (a_{11}^t - b_{11}^t) \\
a_{32} &= -\frac{g}{2\sqrt{2}}
\end{aligned}$$

References

- [1] For an introduction to supersymmetry, see J. Wess and J. Bagger, *Supersymmetry and Supergravity* (Princeton University Press, 1983); P. Fayet and S. Ferrara, Phys. Rep.

- 32**, 249 (1977); P. West, *Introduction to Supersymmetry and Supergravity* (World Scientific, 1986); R.N. Mohapatra, *Unification and Supersymmetry* (Springer-Verlag, 1986).
- [2] For phenomenological reviews of SUSY, see H.P. Nilles, Phys. Rep. **110**, 1 (1984); G.G. Ross, *Grand Unified Theories* (Benjamin Cummings, 1985); R. Arnowitt, A. Chamseddine and P. Nath, *Applied N = 1 Supergravity* (World Scientific, 1984); H. Haber and G. Kane, Phys. Rep. **117**, 75 (1985); J. Bagger, lectures at TASI 1995 (to be published)
- [3] X. Tata, lectures at TASI 1995 (to be published), UH-511-833-95, hep-ph/9510287
- [4] A. Bartl, H. Fraas, W. Majerotto and N. Oshimo, Phys. Rev. **D40**, 1594 (1989); A. Bartl, H. Fraas, W. Majerotto and B. Mösslacher, Z. Phys. **C55**, 257 (1992).
- [5] J. Ellis, S. Rudaz, Phys. Lett. **B218**, 248 (1983); J. F. Gunion, H. E. Haber, Nucl. Phys. **B272**, 1 (1986).
- [6] J.-F. Grivaz, Rapporteur Talk, International Europhysics Conference on High Energy Physics, Brussels, 1995; ALEPH collaboration, CERN-PPE/96-10, submitted to Phys. Lett. **B** (1996). H. Nowak and A. Sopczak, L3 Note 1887, Jan. 1996 ; S. Asai and S. Komamiya, OPAL Physics Note PN-205, Feb. 1996
- [7] K. Hikasa and M. Kobayashi, Phys. Rev. **D36**, 724 (1987).
- [8] H. Baer, M. Drees, R. Godbole, and X. Tata, Phys. Rev. **D44**, 725 (1991), H. Baer, J. Sender, and X. Tata, Phys. Rev. **D50**, 4517 (1994).
- [9] S. Abachi et al., Phys. Rev. Lett. **76**, 2222 (1996)
- [10] A. Bartl, H. Eberl, S. Kraml, M. Majerotto and W. Porod, UWThPh-1996-35, HEPHY-PUB 646/96, hep-ph/9605412.
- [11] A. Denner, H. Eck, O. Hahn, J. Küblbeck, Nucl. Phys. **B 387**, 467 (1992).

Figure Captions

Fig. 1:

Feynman graphs for the decay $\tilde{t}_1 \rightarrow bW\tilde{\chi}_1^0$ related to the matrix elements $\mathcal{M}_{1,i=1,2}$, $\mathcal{M}_{2,i=1,2}$ and \mathcal{M}_3 eq. (7)–eq. (9). The arrow of the fermionic lines defines a fermion flow and is not necessarily identical with the momentum flow used in our calculations.

Fig. 2:

Regions in the $\mu - M_2$ plane for $m_{\tilde{\chi}_1^+} + m_b > m_{\tilde{t}_1} > m_{\tilde{\chi}_1^0} + m_b + m_W$ for $m_W = 80$ GeV, $m_b = 5$ GeV, (I) $m_{\tilde{t}_1} = 220$ GeV and (II) $m_{\tilde{t}_1} = 170$ GeV. Fig.a) is for the case $\tan\beta = 2$, whereas b) shows the case $\tan\beta = 30$. The shaded region will be probed by LEP2 assuming that signals from charginos with a mass smaller than 90 GeV will be observable there.

Fig. 3:

Total width for the decay $\tilde{t}_1 \rightarrow bW\tilde{\chi}_1^0$ for $m_{\tilde{t}_1} = 220$ GeV. Fig.a) shows the width as a function of $\tan\beta$ for $\cos\theta_t = 0.7$ and Fig.b) that of $\cos\theta_t$ for $\tan\beta = 20$. We have taken $M_2 = 250$ GeV and different values of μ : $\mu = -750$ GeV (solid line), $\mu = 750$ GeV (short dashed line), $\mu = -500$ GeV (long dashed line) and $\mu = 500$ GeV (dotted dashed line). The other parameters are given in the text.

Fig. 4:

Total width for the decay $\tilde{t}_1 \rightarrow bW\tilde{\chi}_1^0$ as a function of $\cos\theta_t$ for $m_{\tilde{t}_1} = 170$ GeV. The parameters (see also tab.1) are for a) (solid line) $\mu = -500$ GeV, $M_2 = 165$ GeV and $\tan\beta = 2$, for b) (short dashed line) $\mu = 500$ GeV, $M_2 = 165$ GeV and $\tan\beta = 2$, for c) (long dashed line) $\mu = -1000$ GeV, $M_2 = 166$ GeV and $\tan\beta = 30$ and for d) (dotted-dashed line) $\mu = 1000$ GeV, $M_2 = 167$ GeV and $\tan\beta = 30$.

Fig. 5:

The branching ratios for the decays $\tilde{t}_1 \rightarrow bW\tilde{\chi}_1^0$ (solid line) and $\tilde{t}_1 \rightarrow c\tilde{\chi}_1^0$ (dashed line) for $m_{\tilde{t}_1} = 220$ GeV, $M_2 = 250$ GeV and $\mu = -500$ GeV. The other parameters are explained in the text. Fig. a shows the dependence on $\tan\beta$ whereas Fig. b shows the dependence on $\cos\theta_t$.

Fig. 6:

The branching ratios for the decays $\tilde{t}_1 \rightarrow bW\tilde{\chi}_1^0$ (solid line) and $\tilde{t}_1 \rightarrow c\tilde{\chi}_1^0$ (dashed line) for $m_{\tilde{t}_1} = 170$ GeV and all other parameters as in Fig. 4 (see also tab.1). In case of scenario c) we also show the branching ratio for the (in this case accessible) decay $\tilde{t}_1 \rightarrow c\tilde{\chi}_2^0$ (dotted-dashed line). Notice that we dropped scenario d) due to the fact that there are no visible differences between the scenarios c) and d).

Tabular 1

scenario	μ	M_2	$\tan \beta$	$m_{\tilde{\chi}_1^0}$	$m_{\tilde{\chi}_2^0}$	$m_{\tilde{\chi}_1^\pm}$
a)	-500	165	2	84.4	171.8	171.7
b)	500	165	2	83.4	169.2	169.2
c)	-1000	166	30	82.6	165.4	165.4
d)	1000	167	30	82.8	165.5	165.5

Tabular caption:

Parameters used in the scenarios for the case $m_{\tilde{t}_1} = 170$ GeV. Additionally we show the respective values for the masses (in GeV) of the two lighter neutralinos and the lighter chargino. The other parameters are fixed at $M_Q = M_D = 500$ GeV and $A_b = -350$ GeV.

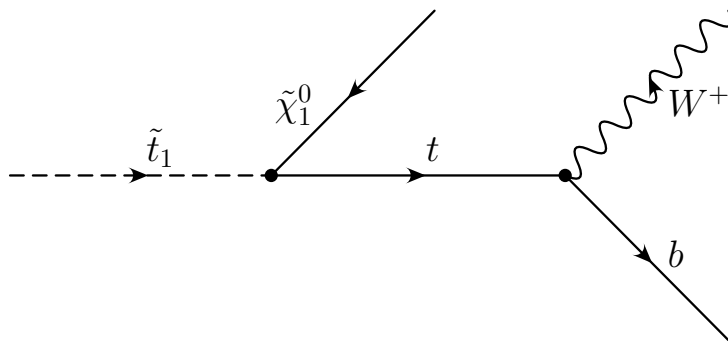
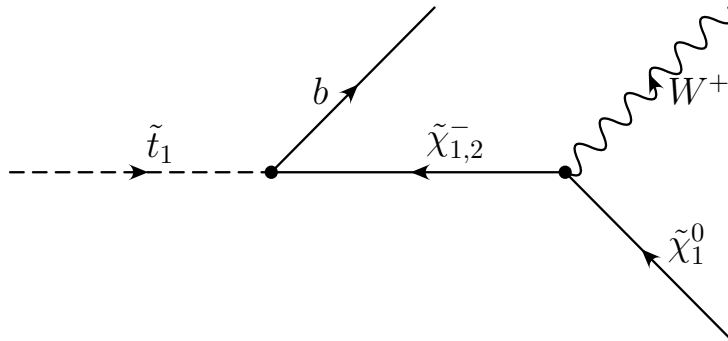
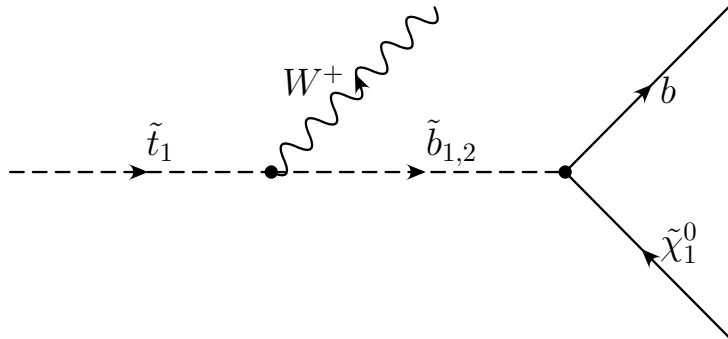


Fig. 1

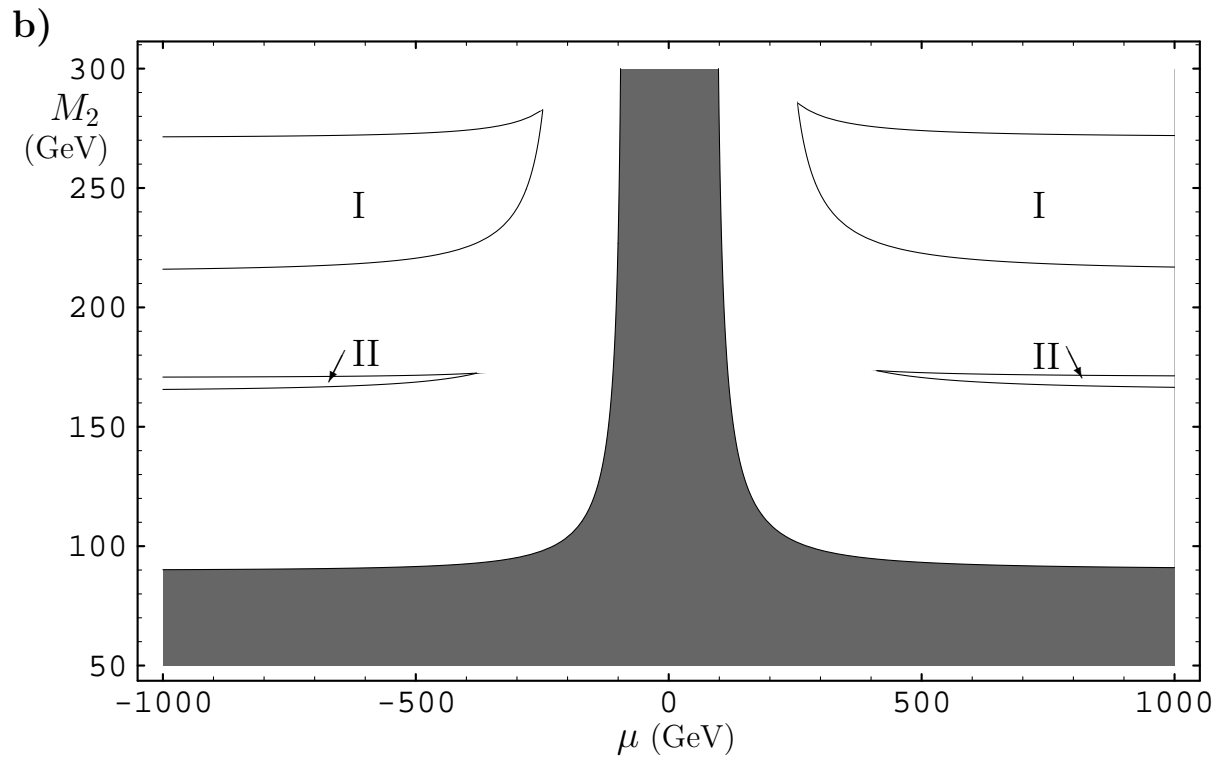
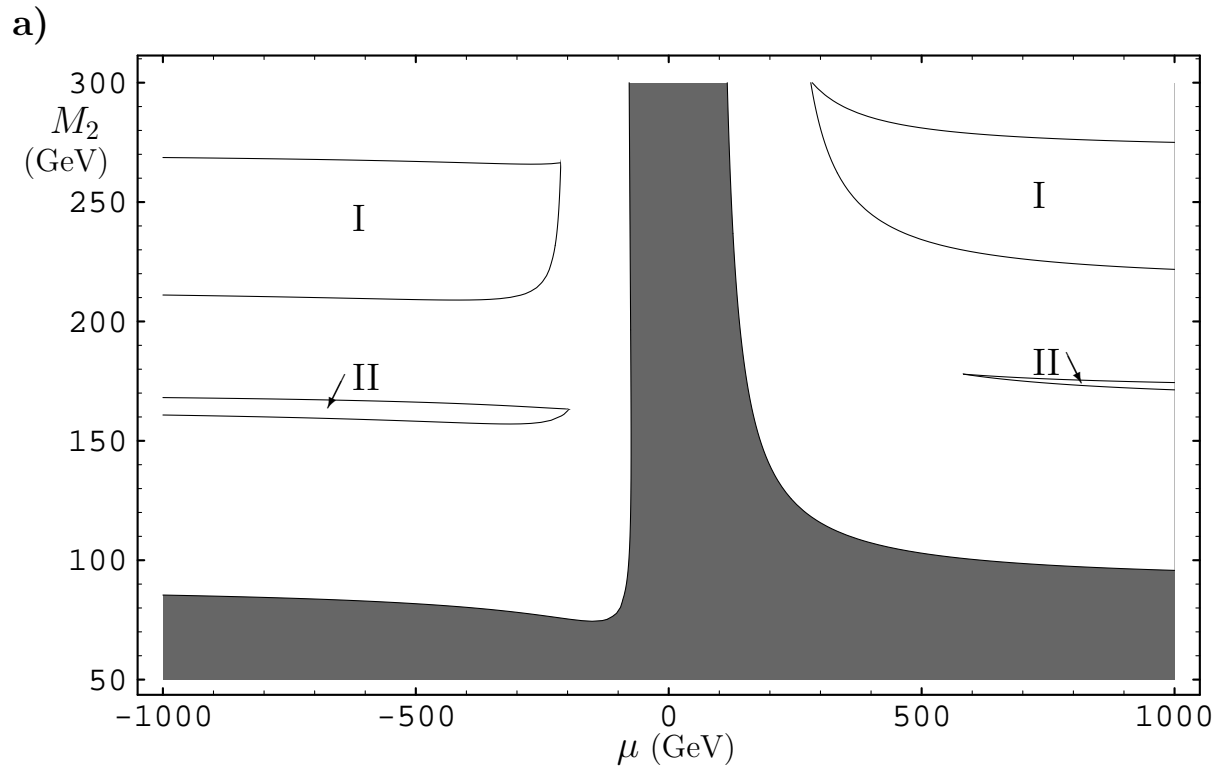


Fig. 2

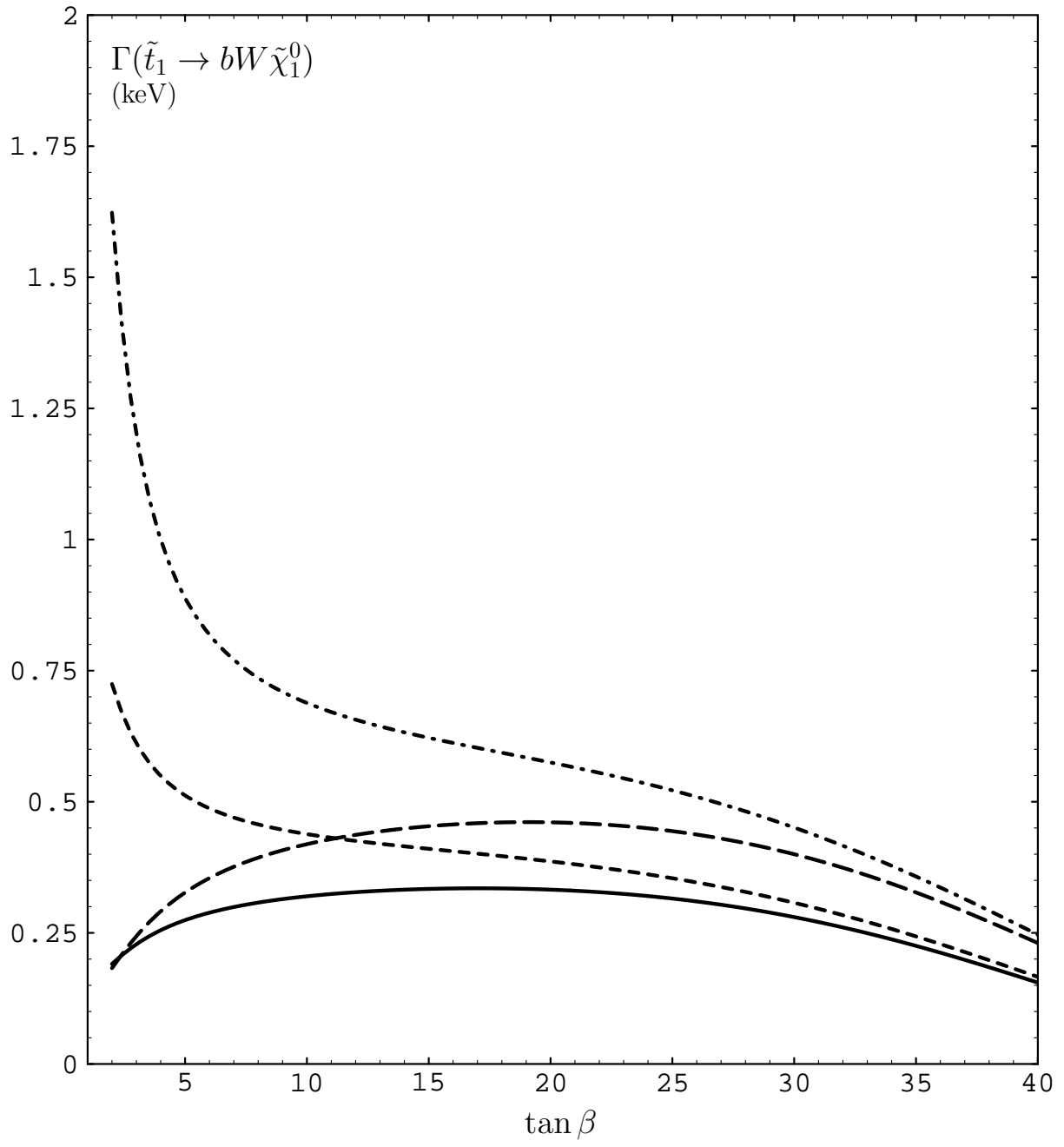


Fig. 3a

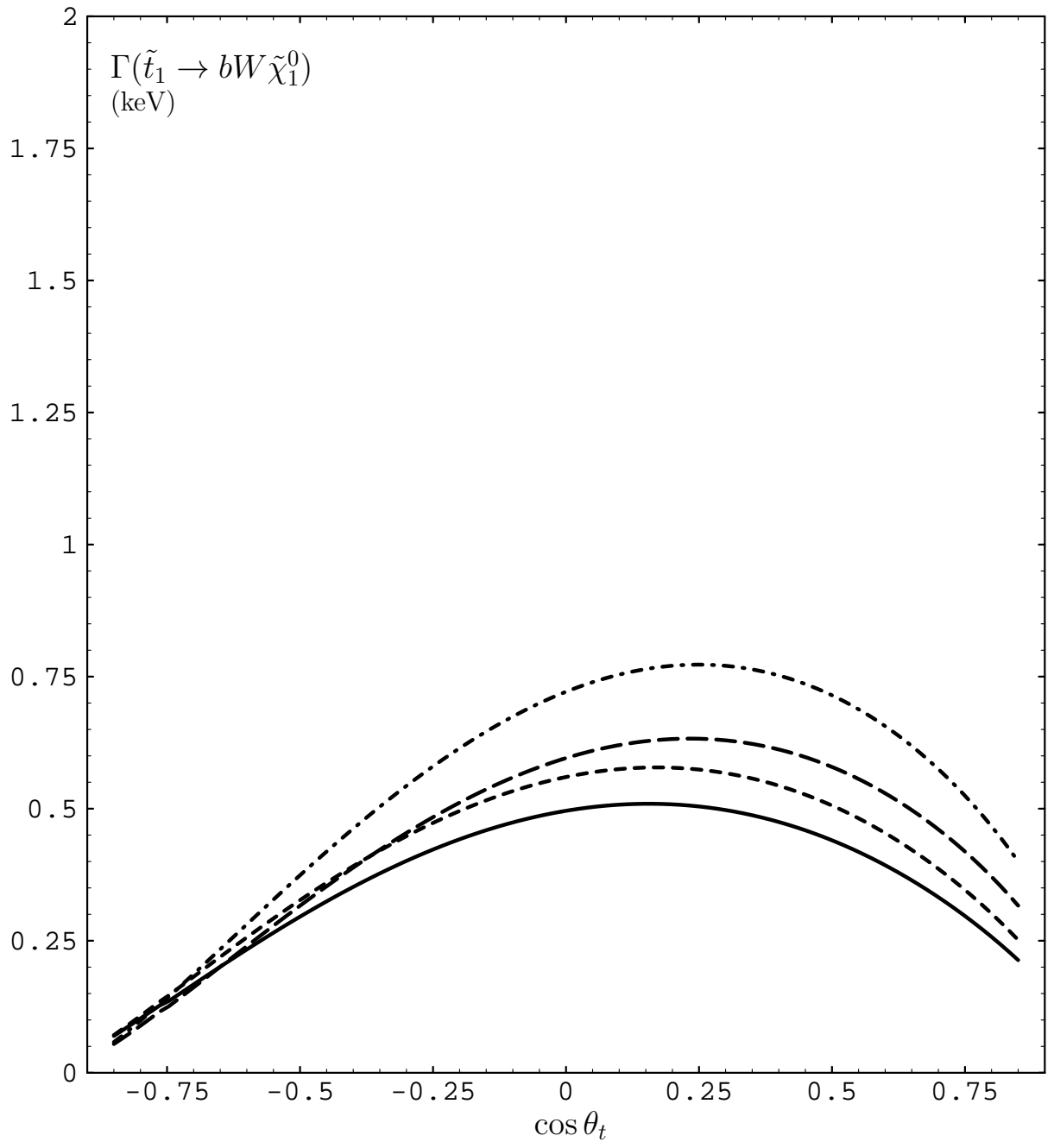


Fig. 3b

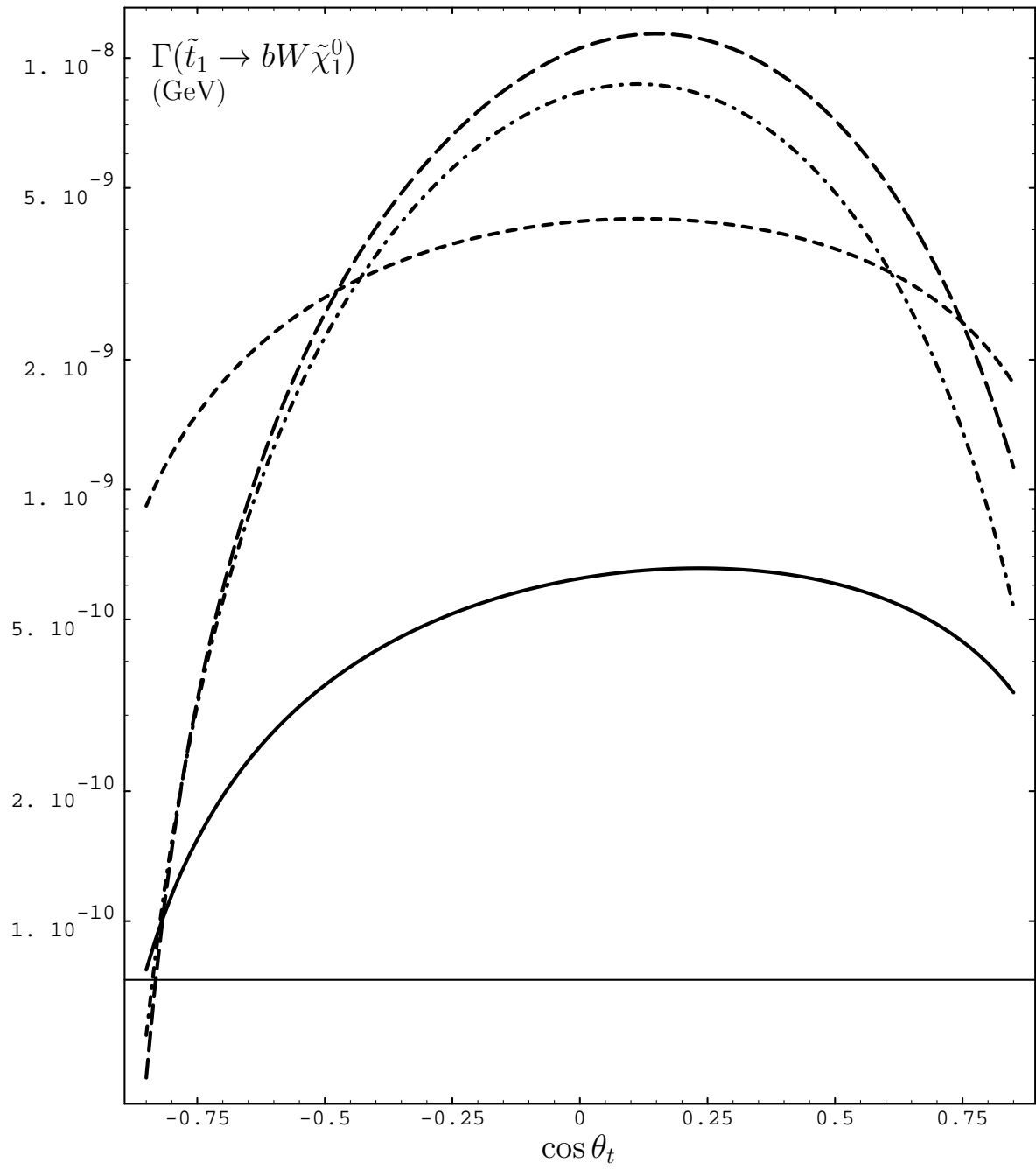


Fig. 4

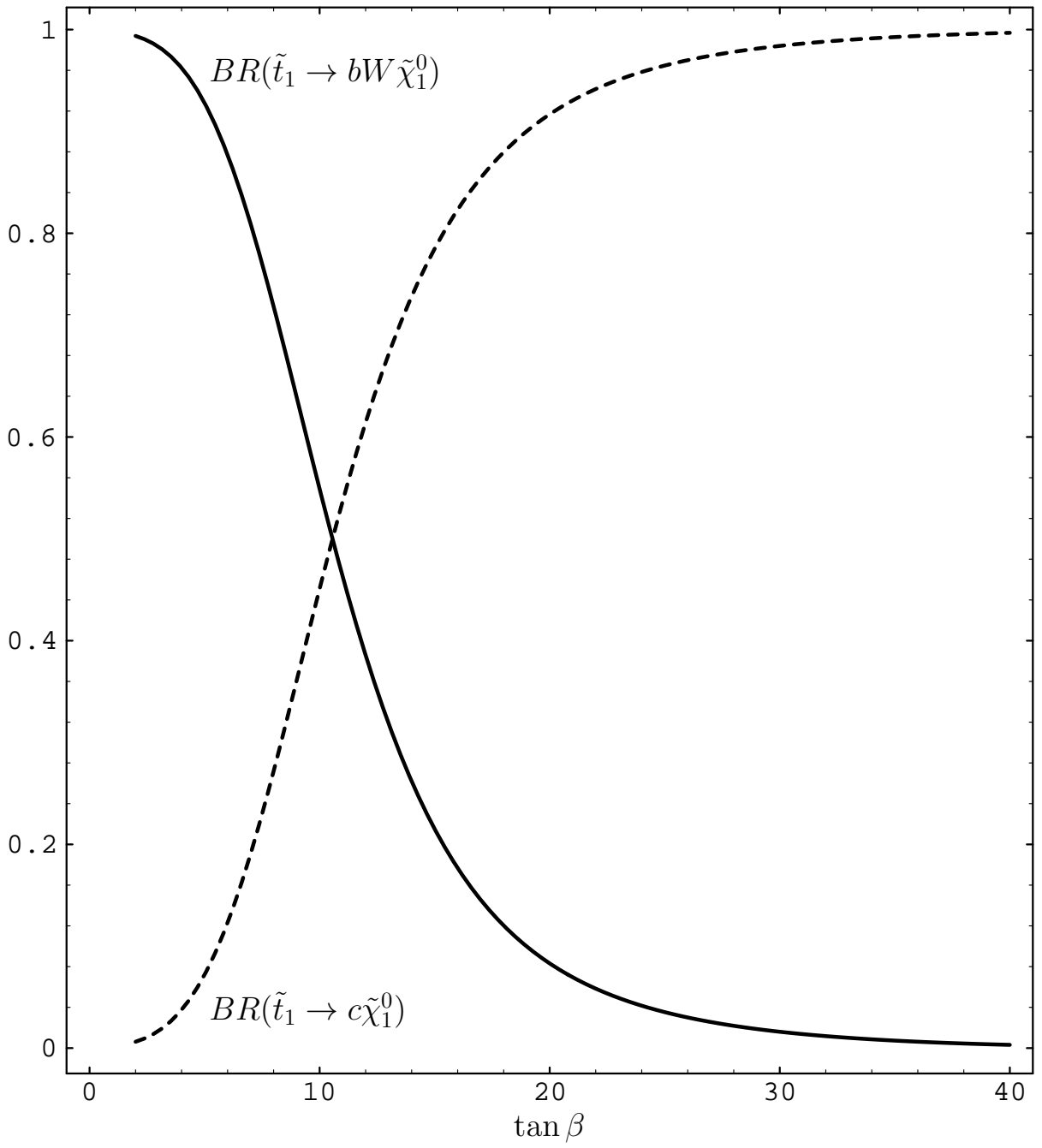


Fig. 5a

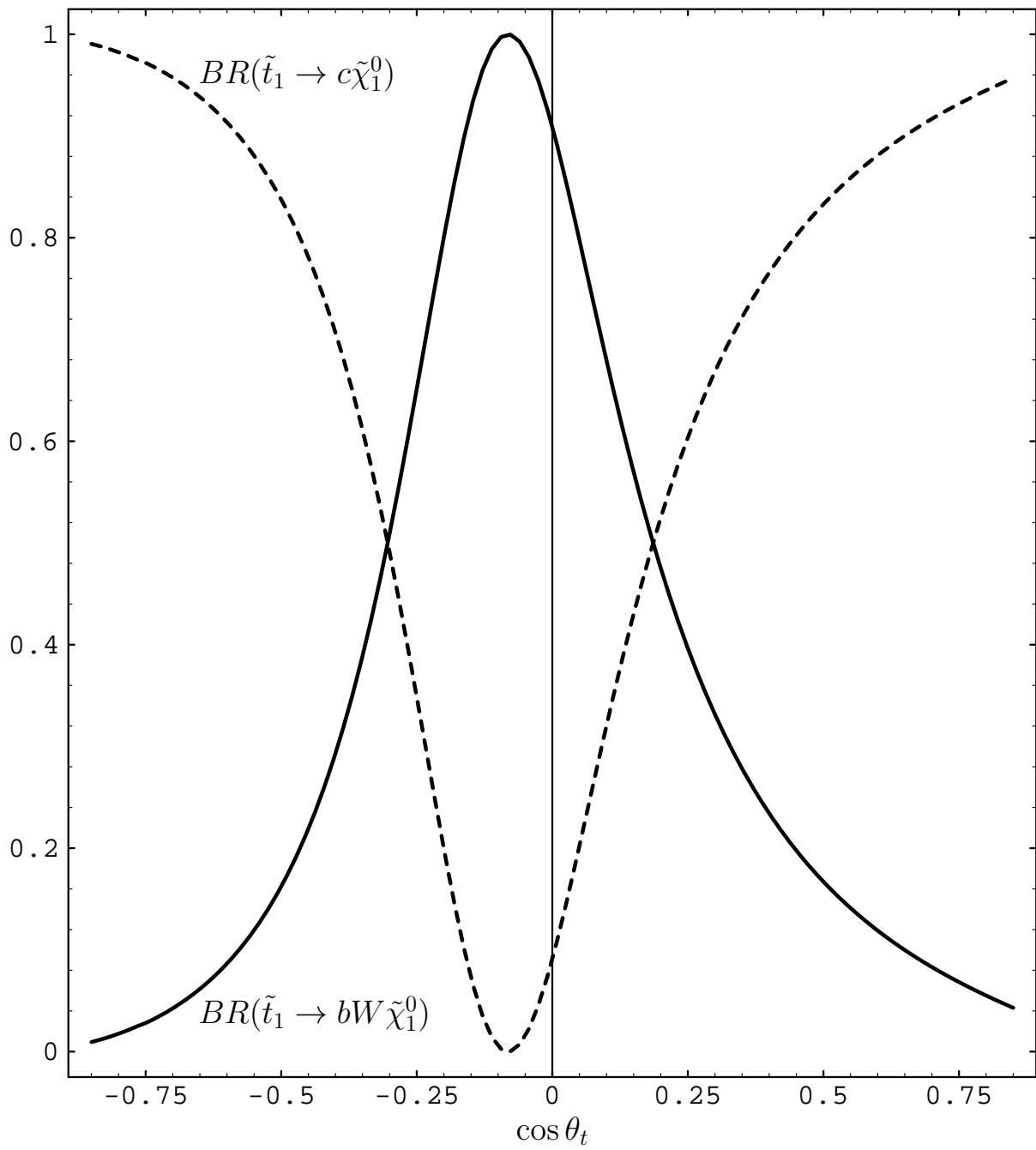


Fig. 5b

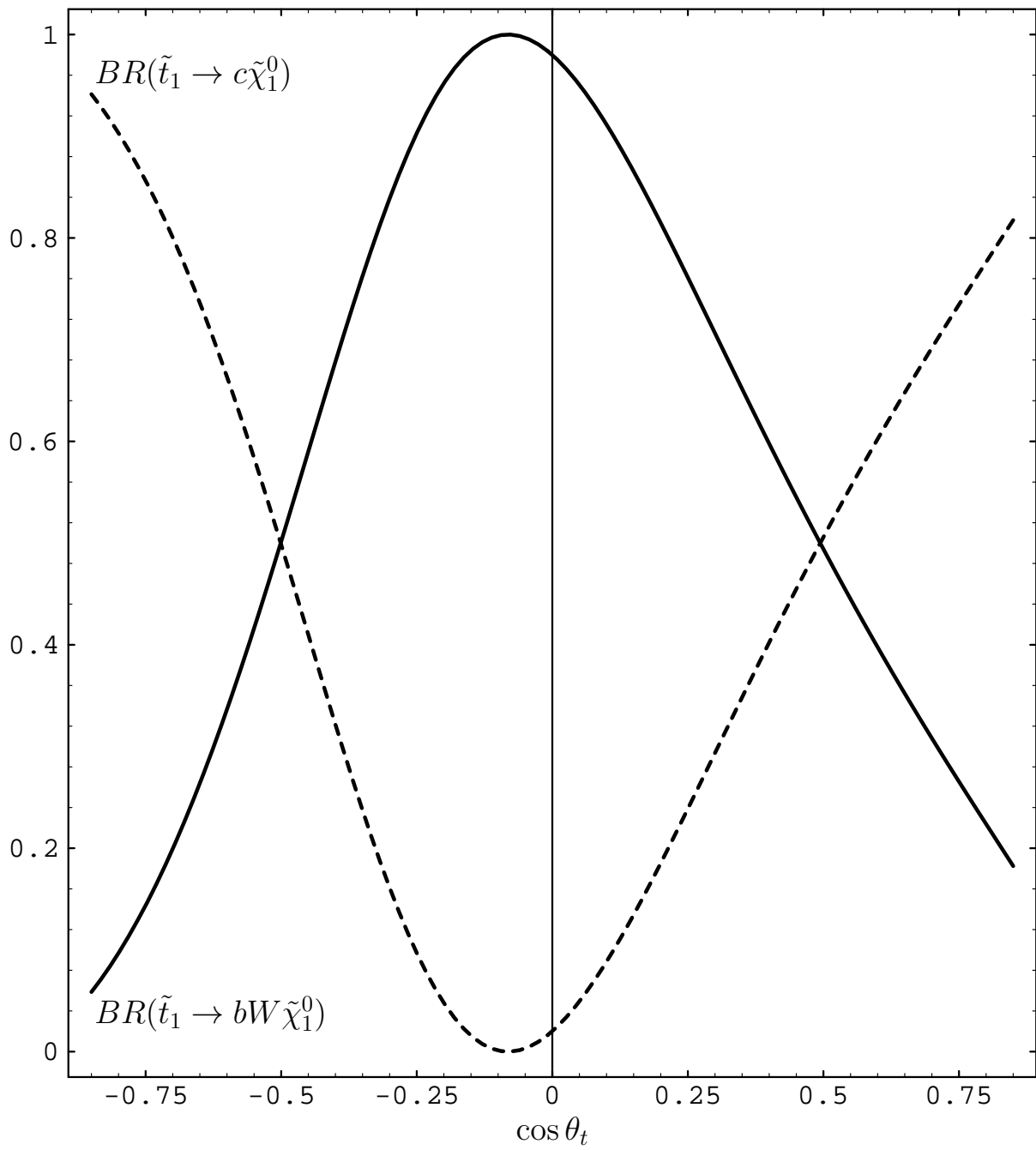


Fig. 6a

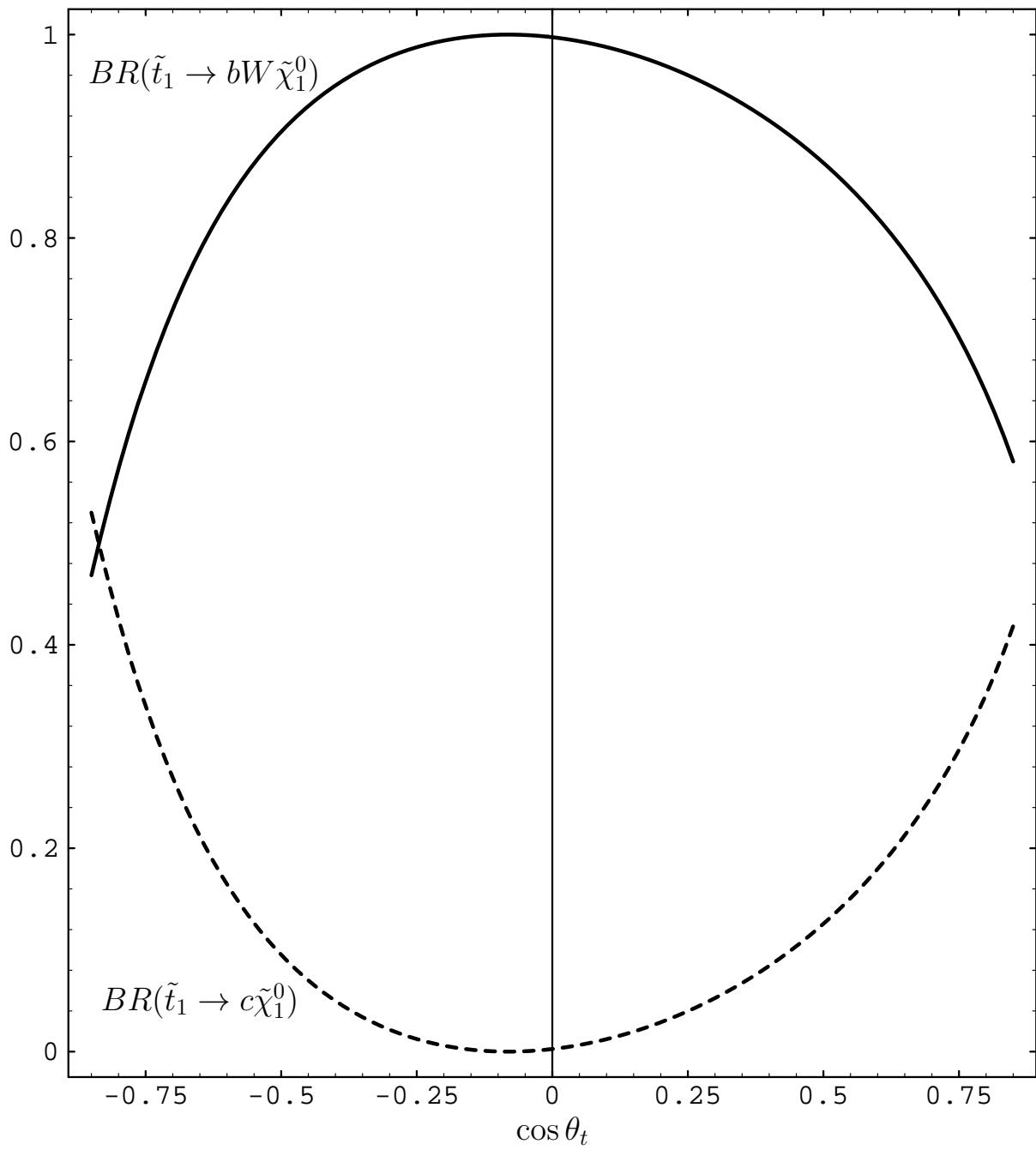


Fig. 6b

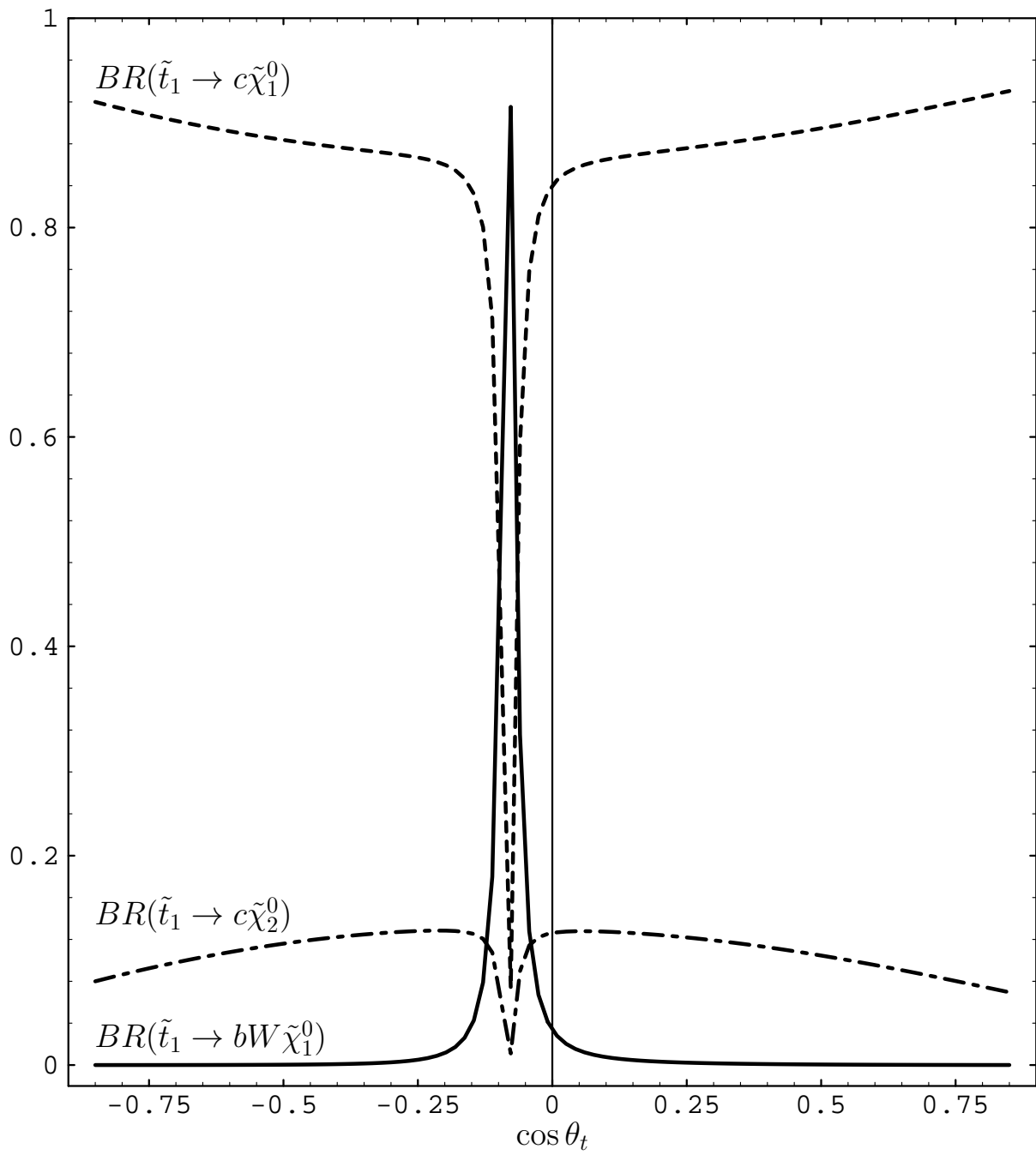


Fig. 6c